The Astrophysical Journal, 716:1397–1407, 2010 June 20 doi:10.1088/0004-637X/716/2/1397

SUPERMASSIVE DARK STARS: DETECTABLE IN *JWST*

Katherine Freese[1], Cosmin Ilie[1], Douglas Spolyar[2], Monica Valluri[3], and Peter Bodenheimer[4]
[1] Michigan Center for Theoretical Physics, Department of Physics, University of Michigan, Ann Arbor, MI 48109, USA
[2] Center for Particle Astrophysics, Fermi National Accelerator Laboratory, Batavia, IL 60510, USA
[3] Department of Astronomy, University of Michigan, Ann Arbor, MI 48109, USA
[4] UCO/Lick Observatory, Department of Astronomy and Astrophysics, University of California, Santa Cruz, CA 95064, USA
Received 2010 February 13; accepted 2010 April 25; published 2010 June 2

ABSTRACT

The first phase of stellar evolution in the history of the universe may be dark stars (DSs), powered by dark matter (DM) heating rather than by nuclear fusion. Weakly interacting massive particles (WIMPs), which may be their own antipartners, collect inside the first stars and annihilate to produce a heat source that can power the stars for millions to billions of years. In this paper, we show that these objects can grow to be supermassive dark stars (SMDSs) with masses $\gtrsim(10^5$–$10^7)\,M_\odot$. The growth continues as long as DM heating persists, since DSs are large and cool (surface temperature $\lesssim 5\times10^4$ K) and do not emit enough ionizing photons to prevent further accretion of baryons onto the star. The DM may be provided by two mechanisms: (1) gravitational attraction of DM particles on a variety of orbits not previously considered and (2) capture of WIMPs due to elastic scattering. Once the DM fuel is exhausted, the SMDS becomes a heavy main-sequence star; these stars eventually collapse to form massive black holes (BHs) that may provide seeds for supermassive BHs in the universe. SMDSs are very bright, with luminosities exceeding $(10^9$–$10^{11})\,L_\odot$. We demonstrate that for several reasonable parameters, these objects will be detectable with the *James Webb Space Telescope*. Such an observational discovery would confirm the existence of a new phase of stellar evolution powered by DM.

Key words: accretion, accretion disks – dark matter – stars: evolution – stars: formation – stars: pre-main sequence

Online-only material: color figures

1. INTRODUCTION

Spolyar et al. (2008) first considered the effect of dark matter (DM) particles powering the first stars. The first stars formed when the universe was about 200 million years old, at $z = 10$–50, in $10^6\,M_\odot$ halos consisting of 85% DM and 15% baryons in the form of H and He from big bang nucleosynthesis; for reviews of the standard picture of the formation of the first stars, see Barkana & Loeb (2001), Yoshida et al. (2003), Bromm & Larson (2004), and Ripamonti & Abel (2005). The canonical example of particle DM is weakly interacting massive particles (WIMPs). In many theories, WIMPs are their own antiparticles and annihilate among themselves wherever the DM density is high. Recently, there has been much excitement in the DM community about possible detections of WIMPs via annihilation to positrons seen by the *PAMELA* satellite (Adriani et al. 2009); annihilation to γ-rays seen by *Fermi* (Abdo et al. 2009; Dobler et al. 2009), and in the direct detection experiments DAMA and CDMS (Bernabei et al. 2010; Ahmed et al. 2009). The annihilation rate is $n_\chi^2\langle\sigma v\rangle$ where n_χ is WIMP density and we take the standard annihilation cross section[5]

$$\langle\sigma v\rangle = 3\times10^{-26}\,\mathrm{cm^3\,s^{-1}}, \quad (1)$$

and WIMP masses in the range 1 GeV–10 TeV. The first stars are particularly good sites for annihilation: they form in the right place—in the high density centers of DM halos—and at the right time—at high redshifts (density scales as $(1+z)^3$). Spolyar et al. (2008) found that above a certain density ($\approx10^{13}$ cm^{-3}) the WIMP annihilation products remain trapped in the star, thermalize with the star, and thereby provide a heat source. These first dark stars (DSs) are stars made primarily of hydrogen and helium with only ∼0.1% of the mass in the form of DM; yet they shine due to DM heating. Note that the term "dark" refers to the power source, not the appearance or the primary matter constituent of the star.

DSs are born with masses $\sim1\,M_\odot$. They are giant puffy (∼10 AU), cool (surface temperatures <10,000 K), yet bright $>10^6\,L_\odot$ objects (Freese et al. 2008a). They reside in a large reservoir ($\sim10^5\,M_\odot$) of baryons, i.e., ∼15% of the total halo mass. These baryons can start to accrete onto the DSs. Previous work (Freese et al. 2008a; Spolyar et al. 2009) followed the evolution of DSs from their inception at $1\,M_\odot$, as they accreted baryons from the surrounding halo, up to $\sim1000\,M_\odot$. DSs can continue to grow in mass as long as there is a supply of DM fuel.

The exciting new development of this paper is that we follow the growth of DSs to become supermassive dark stars (SMDSs) of mass $M_* > 10^5\,M_\odot$. Specifically, we study the formation of $10^5\,M_\odot$ SMDS in $10^6\,M_\odot$ DM halos and $10^7\,M_\odot$ SMDS in $10^8\,M_\odot$ halos; perhaps the SMDSs become even larger. Hoyle & Fowler (1963) first postulated the existence of such large stars but were not aware of a mechanism for making them. Now the confluence of particle physics with astrophysics may be providing the answer. The key ingredient that allows DSs to grow so much larger than ordinary fusion-powered Population III stars is the fact that DSs are so much cooler. Ordinary Population III stars have much larger surface temperatures in excess of 50,000 K. They produce ionizing photons that provide a variety of feedback mechanisms that cut off further accretion. McKee & Tan (2008) have estimated that the resultant Population III stellar masses are $\sim140\,M_\odot$. DSs are very different from fusion-powered stars, and their cooler

[5] Annihilation in the early universe with this value of the cross section leaves behind the correct relic WIMP DM abundance today, ∼24% of the energy density of the universe.

surface temperatures allow continued accretion of baryons all the way up to enormous stellar masses, $M_* > 10^5\,M_\odot$.

WIMP annihilation produces energy at a rate per unit volume

$$\hat{Q}_{\rm DM} = n_\chi^2 \langle \sigma v \rangle m_\chi = \langle \sigma v \rangle \rho_\chi^2 / m_\chi, \quad (2)$$

where n_χ is the WIMP number density, m_χ is the WIMP mass, and ρ_χ is the WIMP energy density. The annihilation products typically are electrons, photons, and neutrinos. The neutrinos escape the star, while the other annihilation products are trapped in the DS, thermalize with the star, and heat it up. The luminosity from the DM heating is

$$L_{\rm DM} \sim f_Q \int \hat{Q}_{\rm DM} dV, \quad (3)$$

where f_Q is the fraction of the annihilation energy deposited in the star (not lost to neutrinos) and dV is the volume element. We take $f_Q = 2/3$ as is typical for WIMPs.

Typically (100–10^4) $M_\odot$ of DM (up to ~1% of the halo mass) must be consumed by the star in order for large SMDS masses $M_* \sim 10^5\,M_\odot$ to be reached. We will consider two different scenarios for supplying this amount of DM:

1. Extended adiabatic contraction (AC), labeled "without capture" below. In this case, DM is supplied by the gravitational attraction of the baryons in the star. The amount of DM available for DM annihilation due to AC may be larger than our previous estimates which were based on the assumption that DM halos are spherical. In a non-spherical DM halo, the supply of DM available to the star can be considerably enhanced, as we discuss in more detail in Section 2.2. In any case, this mechanism relies solely on the particle physics of WIMP annihilation and does not include capture of DM by baryons (discussed below).
2. Extended capture, labeled "with capture" below. Here, the star is initially powered by the DM from AC, but the AC phase is taken to be short ~300,000 yr; once this DM runs out, the star shrinks, its density increases, and subsequently the DM is replenished inside the star by capture of DM from the surroundings (Freese et al. 2008b; Iocco 2008) as it scatters elastically off of nuclei in the star. In this case, the additional particle physics ingredient of WIMP scattering is required. This elastic scattering is the same mechanism that direct detection experiments (e.g., CDMS, XENON, LUX, DAMA) are using in their hunt for WIMPs. In previous work (Freese et al. 2008a; Spolyar et al. 2009), we assumed minimal capture, where DM heating and fusion contributed equally to the luminosity once the star reached the main sequence. Here, we consider the more sensible case where DM heating dominates completely due to larger ambient DM density, and the star can grow to become supermassive.

SMDSs can result from either of these mechanisms for DM refueling inside the star. The SMDS can live for a very long time, tens to hundreds of million years, or possibly longer (even to today). We find that ~$10^5\,M_\odot$ SMDSs are very bright ~$3 \times 10^9\,L_\odot$, which makes them potentially observable by the *James Webb Space Telescope* (*JWST*). We also note that SMDS may become even more massive (1) if they form in larger halos or (2) the DM halos in which they initially form merge with other halos so that there is even more matter to accrete (note that alternatively these mergers may remove the DS from their high DM homes and stop the DM heating). For example, if DSs form in $10^8\,M_\odot$ halos, then they could in principle grow to contain all the baryons in the halo, i.e., $M_* > 10^7\,M_\odot$. Since the luminosity scales as $L_* \propto M_*$ these SMDSs would be even brighter, $L_* > 10^{11}\,L_\odot$ and are hence even better candidates for discovery in *JWST*.

Once the SMDSs run out of DM fuel, they contract and heat up. The core reaches 10^8 K and fusion begins. As fusion-powered stars they do not last very long before collapsing to black holes (BHs). Again, this prediction is different from standard Population III stars, many of which explode as pair-instability supernovae (Heger & Woosley 2002) with predicted even/odd element abundance ratios that are not (yet) observed in nature. The massive BH remnants of the SMDSs are good candidates for explaining the existence of $10^9\,M_\odot$ BHs which are the central engines of the most distant ($z > 5.6$) quasars in the Sloan Digital Sky Survey (SDSS; Fan et al. 2001, 2004, 2006).[6]

The idea of supermassive DS and the resultant $>10^5\,M_\odot$ BH was originally proposed by Spolyar et al. (2009). Subsequently, Umeda et al. (2009) took their existing stellar codes and added DM annihilation to allow the mass to grow. They started from Population III stars in which fusion was already present, assuming they then encounter a reservoir of DM. Here, we start from the very beginning with collapsing protostellar clouds that transition into DSs, which can be DM powered for millions to billions of years before fusion ever begins. The SMDSs in this paper are primordial supermassive stars. More generally, the capture mechanism in particular lends itself to growth of DSs, whether or not fusion has already set in, so that SMDS can result at various epochs in the universe.

Begelman (2009) presents another alternative for the formation of supermassive stars: rapid accretion onto stars which already have hydrogen burning in them. His "quasistars," another possible route to large BH, are quite different from the SMDS discussed in this paper.

Various other authors that have explored the repercussions of DM heating in the first stars (Taoso et al. 2008; Yoon et al. 2008; Ripamonti et al. 2009; Iocco et al. 2008). Recently, in a paper that appeared after we submitted this work, Ripamonti et al. (2010) study the effects of DM heating on the evolution of primordial gas clouds using a one-dimensional code. We are currently not in disagreement with the basic results of their work. We agree that the cloud continues to shrink to a smaller radius and higher density once dark matter heating dominates over cooling—but not for long, only until it reaches thermal and hydrostatic equilibrium. For example, once our canonical 100 GeV case reaches a central density of 10^{16} cm^{-3}, then our equilibrium dark star begins (and not at a lower density). Such a high density is beyond the reach of the code run by Ripamonti et al. and requires further work.

The possibility that DM annihilation might have effects on *today's* stars was initially considered in the 1980s and early 1990s (Krauss et al. 1985; Bouquet & Salati 1989; Salati & Silk 1989; Graff & Freese 1996) and has recently been studied in interesting papers by Moskalenko & Wai (2007), Scott et al. (2007), Bertone & Fairbairn (2007), and Scott et al. (2009). Other constraints on DS will arise from cosmological considerations. A first study of their effects (and those of the resultant main-sequence stars) on reionization has been done by Schleicher et al. (2008, 2009) and further work in this direction is warranted.

In this paper, we examine the SMDSs that result from the two mechanisms discussed above for DM refueling inside the

[6] We thank N. Yoshida for pointing this out to us.

star. In Section 2, we discuss the procedure for calculation of models; in Section 3 we present results; and in Section 4 we end with a discussion.

2. STRUCTURE AND EVOLUTION OF THE DARK STAR

DM heating is very different from fusion. In order to overcome the Coulomb barriers between nuclei, fusion requires very high temperatures and densities in the star. Fusion is not very efficient in that only <1% of the nuclear mass is converted to heat. WIMP annihilation, on the other hand, takes place at high DM densities regardless of the temperature. It is almost 100% efficient since $O(1)$ of the WIMP mass is converted to useful energy. Thus, in the evolution of the first protostars, DM heating becomes important early. Here, we start the calculation when the DS is massive enough ($3\,M_\odot$) so that it is in hydrostatic equilibrium and most of the hydrogen and helium is ionized. The contribution to DM luminosity is roughly constant as a function of radius throughout the DS, unlike fusion which takes place only at the (high temperature) core of the star.

2.1. Basic Equations

We use the numerical code previously discussed in detail by Freese et al. (2008a) and Spolyar et al. (2009). We make the assumption that a DS can be described as a polytrope

$$P = K\rho^{1+1/n} \tag{4}$$

in hydrostatic equilibrium. Here, P is the pressure, ρ is the density, and K is a constant. We solve the equations of stellar structure with polytropic index n initially 1.5, as appropriate for convective stars, and made a gradual transition to $n = 3$ as the star becomes radiative in the later phases. We require that at each time step during the accretion process the star is in hydrostatic equilibrium,

$$\frac{dP}{dr} = -\rho(r)\frac{GM_r}{r^2}, \tag{5}$$

where $\frac{dM_r}{dr} = 4\pi r^2\rho(r)$, and M_r is the mass enclosed in a spherical shell of radius r. The equation of state includes radiation pressure,

$$P(r) = \frac{k_B\rho(r)T(r)}{m_u\mu} + \frac{1}{3}aT(r)^4 \equiv P_g + P_{\rm rad}, \tag{6}$$

where k_B is the Boltzmann constant, m_u is the atomic mass unit, and $\mu = 0.588$ is the mean atomic weight. The opacity is obtained from a zero metallicity table from OPAL (Iglesias & Rogers 1996) supplemented at low temperatures by opacities from Lenzuni et al. (1991) for $T < 6000$ K. The further assumption is made that the radiated luminosity of the star L_* is balanced by the rate of energy output by all internal sources, $L_{\rm tot}$, as described below in Section 2.3.

$$L_* = 4\pi R_*^2\sigma_B T_{\rm eff}^4 = L_{\rm tot}, \tag{7}$$

where $T_{\rm eff}$ is the surface temperature and R_* is the total radius.

Starting with a mass M and an estimate for the outer radius R_*, the code integrates the structure equations outward from the center. The total rate of energy production $L_{\rm tot}$ is compared to the stellar radiated luminosity, as in Equation (7) and the radius is adjusted until the condition of thermal equilibrium is met (a convergence of 1 in 10^4 is reached).

2.2. Dark Matter Densities

We now describe the two different mechanisms for supplying the DM density.

Extended adiabatic contraction. As the baryons start to collapse into a protostellar cloud at the center of the DM halo, the DM responds to the changing gravitational potential well and falls in as well. As described in our previous work (Spolyar et al. 2008), we will use AC to describe this increase in DM density. For the case of spherical halos, we previously found, by performing exact calculations for comparison (Freese et al. 2009), that the simple Blumenthal method (Blumenthal et al. 1986; Barnes & White 1984; Ryden & Gunn 1987) gives reliable results for the final DM densities up to an unimportant factor of 2; others confirmed this conclusion (Natarajan et al. 2009; Iocco et al. 2008; S. Sivertsson & P. Gondolo 2010, in preparation). Using this simple approach during the AC phase, we found that $\rho_\chi \sim 5\,{\rm GeV\,cm^{-3}}(n_h/{\rm cm^3})^{0.81}$ where n_h is the gas density. These are the values we will use during AC.

In our previous work, we probably underestimated the lifetime of the DM inside the star due to AC. In our previous work, we treated the DM halo as spherical and ran up the DS mass to the point where the DM initially inside the star was entirely consumed by annihilation. The DS mass at this point is $O(10^3)\,M_\odot$ after a lifetime of ~300,000 yr, and the amount of DM consumed has only amounted to $\sim 1\,M_\odot$. In a spherical DM halo, the orbits of DM particles are planar rosettes (Binney & Tremaine 2008) conserving energy as well as all three components of angular momentum; consequently the central hole (or "empty loss cone") that results from DM annihilation cannot be repopulated once it is depleted. (Note that although DM annihilation creates a central hole in the DM density, the entire region is filled with baryons and hence the potential is stable.) However, it is well known that DM halos formed in hierarchical structure formation simulations are not spherical but are prolate-triaxial (Bardeen et al. 1986; Barnes & Efstathiou 1987; Frenk et al. 1988; Dubinski & Carlberg 1991; Jing & Suto 2002; Bailin & Steinmetz 2005; Allgood et al. 2006) with typical axis ratios of (short axis)/(long axis) ~0.6–0.8. In triaxial potentials, the orbits do not conserve angular momentum. In particular, there are two families of "centrophilic orbits" (box orbits and chaotic orbits) which oscillate back and forth through the potential and can travel arbitrarily close to the center (Schwarzschild 1979; Goodman & Schwarzschild 1981; Gerhard & Binney 1985; de Zeeuw 1985; Schwarzschild 1993; Merritt & Fridman 1996; Merritt & Valluri 1996). Unlike an orbit in a spherical potential which has a constant pericenter radius (the distance of closest approach to the center of the potential), the pericenter radius of a centrophilic orbit varies over time extending from $r_{\rm peri} = [0, r_{\rm max}]$ where $r_{\rm max}$ is sometimes referred to as the "throat" of the orbit (Gerhard & Binney 1985). As any one particle traverses the center of the DS, it may indeed be removed from the pool by annihilation. However, it was unlikely to pass through the star (of radius r_*) on its next orbit anyhow since in general $r_{\rm max} \gg r_*$. Instead, a particle on a different "centrophilic orbit" enters the star for the first time maintaining the steady state central DM density cusp. Unlike in the case of a spherical DM halo, where annihilation steadily depletes the central density cusp, in a triaxial halo there is a high probability for a particle on a centrophilic orbit to pass through the center for the first time on any given orbital crossing. This is particularly true in potentials with central point masses which are dominated by chaotic orbits and are therefore ergodic (Merritt & Valluri

1996; Valluri & Merritt 1998). Hence, the central DM density can remain much higher than we previously expected.

The dynamics of the refilling of the central "loss cone" in the case of spherical and non-spherical collisionless systems has been studied previously in the context of capture of stars by a central BH (Gerhard & Binney 1985; Magorrian & Tremaine 1999; Merritt & Poon 2004). The details of filling rate for the specific case of the DS will be presented separately in a later paper; however, these previous papers showed that in non-spherical systems the loss cone could remain full for a factor of 2 to 10^4 times longer than in the spherical case depending on whether the potential was axisymmetric (Magorrian & Tremaine 1999) or triaxial (Merritt & Poon 2004), respectively. Since DM halos are known to be triaxial this suggests that the duration for which the central hole remains full (i.e., has orbits with the low angular momentum necessary for annihilation) can increase from 300,000 yr to as much as 3×10^9 yr possibly allowing the DS to be detectable by *JWST*.

These more optimistic estimates require that a significant fraction of the orbits in these early DM halos are chaotic and boxlike. One important potential concern with assuming conditions in a triaxial halo is that several studies have shown that the growth of central baryonic components tends to make DM halos more axisymmetric than in purely dissipationless simulations (Dubinski 1994; Evrard et al. 1994; Merritt & Quinlan 1998; Kazantzidis et al. 2004; Debattista et al. 2008; Tissera et al. 2009), and axisymmetric models are generally not expected to contain centrophilic orbit families. However, Valluri et al. (2010) recently showed that when a compact central baryonic component is grown adiabatically inside a triaxial DM halo, the final halo that results from the adiabatic growth of such a baryonic component looks nearly oblate, yet its orbit population can contain a significant fraction of centrophilic orbits, since box orbits preferentially deform their shapes rather than converting to centrophobic tube families. Furthermore, they showed that a significant fraction of the orbits (both box orbits and tube orbits which were traditionally thought to avoid the center) experience strong chaotic scattering, a mechanism that could drive them close to the center. They found that for a fixed ratio of the mass of the baryonic component to mass of the DM halo ($M_*/M_{\rm DM} = 10^{-3}$), the smaller the radius of the baryonic component (r_*), relative to the virial radius of the DM halo ($r_{\rm vir}$) the greater was the fraction of chaotic orbits. The most compact baryonic component studied by them had $r_*/r_{\rm vir} = 4.6 \times 10^{-4}$, which is significantly larger than that for our fiducial SMDS for which $r_*/r_{\rm vir} = 2 \times 10^{-7}$. The compactness of the baryonic component in the DS relative to its halo is important since Valluri et al. (2010) showed that when the central component became very compact, orbits that were previously thought to be immune to becoming chaotic (the "long-axis tubes" which are important in prolate DM halos) also become chaotic. M. Valluri & K. Freese (2010, in preparation) are currently computing the rate at which the "loss cone" at the center of the SMDS will be refilled for a range of possible halo and DS masses.

It is interesting to speculate that the initial mass function of the first stars may be determined by the cutoff of the DM supply, which will take place at different SMDS masses in different halos, depending on the details of the cosmological merger history. As the SMDS mass becomes a significant fraction of the halo mass (∼5%–10%), it can significantly affect the shape of the halo, causing it to become more axisymmetric (Merritt & Quinlan 1998) and thereby potentially cutting off the DM supply; on the other hand, in the meantime the halo is growing larger due to mergers, which will replenish the population of radial orbits. Numerical simulations with better resolution than currently possible will be necessary to address these questions.

In the meantime, in our case without capture, we assume that the required DM is present and allows the stellar mass to grow to the point where most of the baryonic content of the initial halo is inside a single SMDS.

The amount of DM required inside the star to sustain DM heating long enough to reach a $10^5\ M_\odot$ SMDS is still small, $\sim 100\ M_\odot$ for accretion rate $\dot{M} = 10^{-2}\ M_\odot\ {\rm yr}^{-1}$ and $\sim 10^4\ M_\odot$ for accretion rate $\dot{M} = 10^{-3}\ M_\odot\ {\rm yr}^{-1}$, out of a total $10^6\ M_\odot$ halo. In the code, we accomplish this by not removing annihilated DM from the pool. More precise studies must be performed later in which we follow individual particle orbits in triaxial potentials to better determine the precise DM density at any one time.

Extended capture. In our model labeled "with capture," we assume (as in our previous papers) that the DM due to AC runs out in ∼300,000 yr. For a while DM heating becomes unimportant and the DS has to contract to maintain pressure support. Then DS is refueled in the later stages due to capture of further DM from the ambient medium. This refueling requires an additional piece of particle physics: scattering of DM off the nuclei inside the star.

Some of the WIMPs from the ambient medium that have orbits passing through the star will eventually be captured and sink to the center, where they can annihilate efficiently. The capture process is irrelevant during the early evolutionary stage of the DS, since the baryon density is not high enough at that point, leading to very small scattering probabilities. However, once the DS approaches the main sequence, the baryon densities become high enough for substantial capture to be possible. This mechanism was first noticed by Freese et al. (2008b) and Iocco (2008).

In our previous work (Spolyar et al. 2009), we investigated a "minimal capture" case which did not cause the DS to grow much more massive than the original case without capture $\sim 1000\ M_\odot$; but we stated our intention to work out the case of a more substantial background DM density in which case the DS would end up supermassive. This is what we investigate here. The capture rate is sensitive to the product of two uncertain quantities: the scattering cross section of WIMP interactions with the nuclei σ_c and the ambient DM density $\bar{\rho}_\chi$. Since the capture mechanism depends only on the product of these two quantities, one can interchangeably vary either of these. For illustration purposes, we will fix $\sigma_c = 10^{-39}\,{\rm cm}^2$ and vary $\bar{\rho}_\chi = (10^{10}$–$10^{14})\,{\rm GeV\,cm}^{-3}$. The latter quantity is the largest reasonable amount based on our results for AC at the DS surface; and the former is the "minimal capture" value considered in all our previous papers. Our fiducial cross section is just below the experimental bound for spin-dependent (SD) scattering; the bound on spin-independent (SI) scattering is much tighter: $\sigma_{c,{\rm SI}} < 3.8 \times 10^{-44}\ {\rm cm}^2$ for $m_\chi = 100$ GeV (Ahmed et al. 2009). We will show that capture can produce sufficient DM in the star to keep DM heating alive for a long time. The details of our procedure for including capture have previously been presented in Spolyar et al. (2009) and will not be repeated here.

2.3. Energy Sources

There are four possible contributions to the DS luminosity:

$$L_{\rm tot} = L_{\rm DM} + L_{\rm grav} + L_{\rm nuc} + L_{\rm cap}, \quad (8)$$

from DM annihilation, gravitational contraction, nuclear fusion, and captured DM, respectively. The heating due to DM

annihilation in Equations (2) and (3) dominates from the time of DS formation until the adiabatically contracted DM runs out. As described previously, in our "without capture" models this stage never ends due to extended AC. In the models "with capture," on the other hand, we take this phase to end after ~300,000 yr, so that the DS has to contract in order to maintain pressure support. The contribution $L_{\rm grav}$ due to gravitational energy release is calculated as in Spolyar et al. (2009). As the DS contracts, the density and temperature increase to the point where nuclear fusion begins. We include deuterium burning starting at $T \sim 10^6$ K, hydrogen burning via the equilibrium proton–proton cycle (Bahcall 1989), and helium burning via the triple-alpha reaction (Kippenhahn & Weigert 1990). During the later stages of the pre-main-sequence evolution in the cases "with capture," the DS becomes dense enough to capture DM from the ambient medium via elastic scattering. Already before fusion can begin, and possibly again after the onset of fusion, captured DM can provide an important energy source with accompanying luminosity

$$L_{\rm cap} = 2m_\chi \Gamma_{\rm cap} = 2m_\chi f_Q \int dV \rho_{\rm cap}^2 \langle \sigma v \rangle / m_\chi^2 \qquad (9)$$

and again $f_Q = 2/3$.

3. RESULTS OF STELLAR STRUCTURE ANALYSIS

Using our polytropic model for DSs, we have started with 3 $M_\odot$ stars and allowed baryonic matter to accrete onto them until they become supermassive with $M_* > 10^5\, M_\odot$. We display results for the case without capture (but with extended AC) as well as the case with capture for a variety of WIMP masses $m_\chi =$ 10 GeV, 100 GeV, and 1 TeV. We have run models for a variety of accretion rates of baryons onto the star including constant accretion rates of $\dot{M} = 10^{-1}, 10^{-2}, 10^{-3}\, M_\odot$ yr^{-1}. We will present results for $\dot{M} = 10^{-3}\, M_\odot$ yr^{-1}, which is approximately the average rate calculated by Tan & McKee (2004) and by O'Shea & Norman (2007).

Our stellar evolution results can be seen in the Hertzsprung–Russell (H-R) diagram of Figure 1 for the case of a $10^6\, M_\odot$ halo. The DS travels up to increasingly higher luminosities as it becomes more massive due to accretion. We have labeled a sequence of ever larger masses until all the baryons (150,000 $M_\odot$) in the original halo are consumed by the SMDS. As the mass increases, so do the luminosity and the surface temperature. In the cases "without capture," the radius increases continuously until all the baryons have been eaten. In the cases "with capture," we have taken the (overly conservative) assumption that the DM from AC is depleted after ~300,000 yr as in our earlier papers; then the luminosity plateaus for a while the DS contracts until eventually it is dense enough to capture further DM.

We note that, for the case "without capture," the H-R diagram is unchanged by varying the accretion rate: only the time it takes to get from one mass stage to the next changes, but the curves we have plotted apply equally to all accretion rates. Similarly, given m_χ, the following quantities are the same regardless of accretion rate: R_*, $T_{\rm eff}$, ρ_c, and T_c.

In a beautiful paper, Hoyle & Fowler (1963) studied supermassive stars in excess of $10^3\, M_\odot$ and found results germane to our work. They treated these as $n = 3$ polytropes (just as we do) dominated by radiation pressure, and found the following results: $R_* \sim 10^{11}(M_*/M_\odot)^{1/2}(T_c/10^8\ {\rm K})^{-1}$ cm, $L_*/L_\odot \sim 10^4 M_*/M_\odot$, and $T_{\rm eff} \sim 10^5 (T_c/10^8\ {\rm K})^{1/2}$ K. While

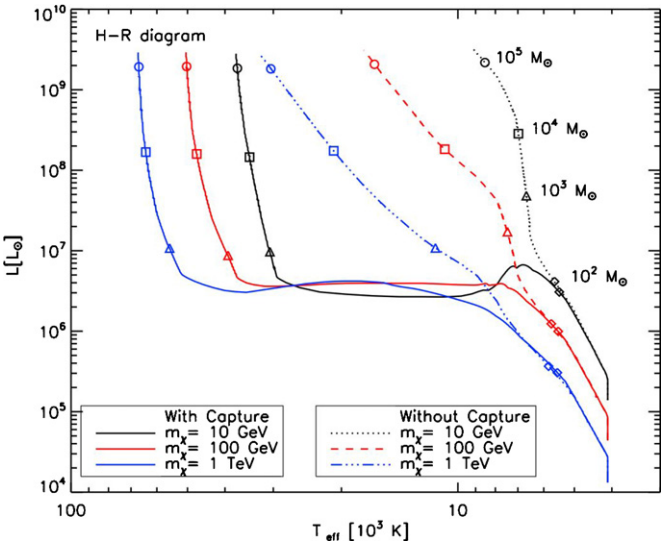

Figure 1. Hertzsprung–Russell diagram of dark stars for accretion rate $\dot{M} = 10^{-3}\, M_\odot$ yr^{-1} and a variety of WIMP masses as labeled for the two cases: (1) "without capture" but with extended adiabatic contraction (dotted lines) and (2) "with capture" (solid lines). The case with capture is for product of scattering cross section times ambient WIMP density $\sigma_c \bar{\rho}_\chi = 10^{-39}\,{\rm cm}^2 \times 10^{13}$ GeV cm^{-3}. Also labeled are stellar masses reached by the DS on its way to becoming supermassive. The final DS mass was taken to be $1.5 \times 10^5\, M_\odot$ (the baryonic mass inside the initial halo), but could vary from halo to halo, depending on the specifics of the halo mergers.

(A color version of this figure is available in the online journal.)

some of the details of their calculations differ from ours, taking the central temperature appropriate to DS in the above relations roughly reproduces our results (to $O(1)$). For example, by using the temperature appropriate to DSs with extended AC ($T_c \sim 10^6$ K) rather than the much higher central temperature ($T_c > 10^8$ K) appropriate to nuclear power generation, the above relations show that DSs have much larger radii and smaller surface temperatures than fusion-powered stars. We wish to draw particular attention to the fact that luminosity scales linearly with stellar mass, and is independent of power source.

Figure 2 plots the H-R diagram "with capture" for a single WIMP mass of 100 GeV, for $\dot{M} = 10^{-3}\, M_\odot$ yr^{-1}, and for $\sigma_c = 10^{-39}$ cm^2, but for a variety of ambient densities ranging from $\bar{\rho}_\chi = (10^{10}$–$10^{14})$ GeV cm^{-3}. The latter is the density one finds due to AC at the photosphere of the DS, and seems the largest sensible starting point for the value of the ambient density. Our previous paper (Spolyar et al. 2009) considered the case of minimal capture with 10^{10} GeV cm^{-3}, which was artificially chosen so that the growth of the DS ceases at 680 $M_\odot$, the radius shrinks, and then fusion and DM heating play equal roles. For ambient densities below 5×10^{10} GeV cm^{-3}, the DS mass growth shuts off well before the star becomes supermassive for the following reason. The cases with capture all take place at higher stellar densities than the cases without; the density must be high enough to be able to capture WIMPs. Consequently, the surface temperature is larger and accretion is shut off more easily by radiation coming from the star. The case of ambient density 10^{10} GeV cm^{-3} (from our previous paper) is a very carefully chosen (delicate) situation. On the low side of this density, DM heating is completely irrelevant and fusion tells the whole story; on the other hand, for any density $\bar{\rho}_\chi \geqslant$ few $\times\, 10^{10}$ GeV cm^{-3}, DM heating is so dominant over fusion that the DS can just continue growing in mass. At these higher densities, the surface temperature never becomes hot enough (≈100,000 K) for feedback effects from the star to cut off

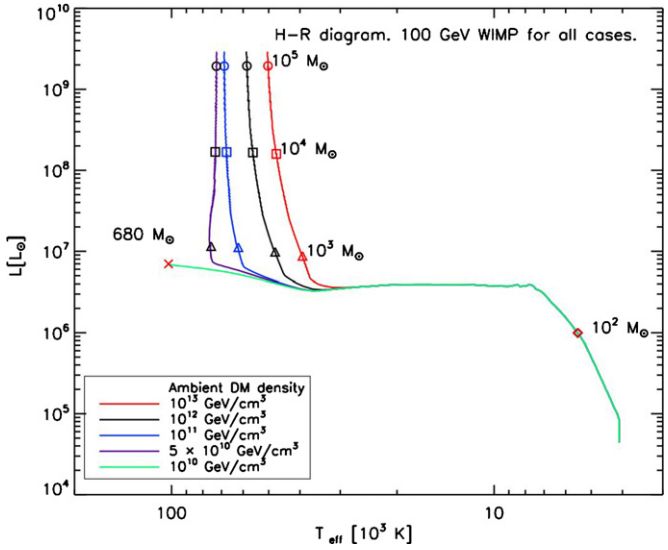

Figure 2. Hertzsprung–Russell diagram of DS for the case "with capture" for 100 GeV WIMP mass and accretion rate $\dot{M} = 10^{-3}\,M_\odot\ \mathrm{yr}^{-1}$. The different curves are for a variety of ambient DM densities $\bar{\rho}_\chi$ as labeled for scattering cross section $\sigma_c = 10^{-39}\ \mathrm{cm}^2$. The results depend only on the product $\sigma_c\bar{\rho}_\chi$ so the different curves could equivalently refer to different σ_c for a given $\bar{\rho}_\chi$.

(A color version of this figure is available in the online journal.)

accretion. Between 50,000 K and 100,000 K, feedback effects are included, and they act to reduce the accretion rate, but they never shut it off entirely for densities above $5 \times 10^{10}\ \mathrm{GeV\ cm}^{-3}$. In reality, a star that is moving around can sometimes hit pockets of high $\bar{\rho}_\chi$ (where it is DM powered and grows in mass) and sometimes hit pockets of low $\bar{\rho}_\chi$ (where fusion takes over). As long as the ambient density remains at least this large, the star can reach arbitrarily large masses and eat the entire baryonic content of the halo.

As described previously, the capture mechanism depends on the product of scattering cross section times ambient density, $\sigma_c\bar{\rho}_\chi$, rather than on either of these quantities separately. Hence, our current discussion could trade off ambient density versus cross section. For example, the product is the same for $\bar{\rho}_\chi = 5 \times 10^{10}\ \mathrm{GeV\ cm}^{-3}$ and $\sigma_c = 10^{-39}\ \mathrm{cm}^2$ as it is for $\bar{\rho}_\chi = 10^{14}\ \mathrm{GeV\ cm}^{-3}$ and $\sigma_c = 5 \times 10^{-43}\ \mathrm{cm}^2$. Thus, for the highest reasonable ambient density, the scattering cross section can be several orders of magnitude lower than the experimental upper bound for SD scattering and still provide substantial capture in DS. While the required σ_c is ruled out (Ahmed et al. 2009) for SI scattering at $m_\chi = 100$ GeV, it is below the bounds at low masses $m_\chi \sim 10$ GeV and in this case can lead to significant DM capture in the stars.

Above $\sim 100\,M_\odot$, one can see that the stellar luminosity scales as $L_* \propto M_*$ and is the same for all models for a given stellar mass; this statement is essentially true for all stars no matter the power source. The reason is that at these masses, the star is essentially radiation pressure supported throughout.[7] This same scaling in supermassive stars was already noticed by Hoyle & Fowler (1963). The luminosity essentially tracks (just below) the Eddington luminosity which scales as $L \propto M_*$.

The curves with higher values of WIMP mass m_χ lie to the left of the curves with lower m_χ. This can be understood as follows. The DM heating rate in Equation (1) scales as $Q \propto \rho_\chi^2/m_\chi$. Hence to reach the same amount of heating and achieve the same luminosity, at higher m_χ the DS must be at higher WIMP density, i.e., the stellar radius must be smaller, the DS is hotter, and the corresponding surface temperature $T_{\rm eff}$ is higher. Also, for higher m_χ the amount of DM in the star is smaller since the star is more compact for the same number of baryons but $\rho_\chi \propto n^{0.8}$ where n is the hydrogen density.

Tables 1 and 2 show various stellar properties for a DS that forms in a $10^6\,M_\odot$ DM halo, as the star evolves to higher mass for the case of $m_\chi = 100$ GeV, for the two cases "without" and "with" capture, respectively. While the DM density is a gently decreasing function of radius for the case without capture, it is extremely sharply peaked at the center of the DS for the case "with capture."

One can see that, in the case "without capture," $\sim 10^4\,M_\odot$ of DM must be annihilated away in order for the DS to reach $10^5\,M_\odot$ for accretion rate $\dot{M} = 10^{-3}\,M_\odot$. The time to reach this mass is $\sim$100 Myr. For an alternative faster accretion rate $\dot{M} = 10^{-2}\,M_\odot$, a smaller amount of DM must be annihilated away, $\sim 100\,M_\odot$; then it takes the DS $\sim$ 10 Myr to reach $\sim 10^5\,M_\odot$. The caveat is that the DM orbits must continue to penetrate into the middle of the DS for this length of time in order for the DM abundance and consequent heating to continue; it is the DM heat source that keeps the DS cool enough to allow it to continue to accrete baryons. Additionally, the assumption that baryons continue to accrete onto the DS must continue to hold. Yet, in the time frame required, the original $10^6\,M_\odot$ halo will merge with its neighbors, so that both the baryon and DM densities are disturbed. These mergers could affect the DS in one of two ways: either they provide more baryons and DM to feed the SMDS so that it ends up being even larger, or they disrupt the pleasant high DM environment of the SMDS so that it loses its fuel and converts to an entirely fusion-powered star. Continued growth of the DS is quite plausible since simulations with massive BHs in mergers show that they prefer to sit close to the center of the density distribution or find the center in a short time after the merger.

Someday detailed cosmological simulations will be required to answer this question. Individual DS in different halos may end up with a variety of different masses depending on the details of the evolution of the halos they live in. The case studied in this paper is clearly a simplistic version of the more complicated reality, but illustrates the basic idea that supermassive stars may be created by accretion onto DS, either with or without capture.

Tables 1 and 2 present models for DSs which form in $10^6\,M_\odot$ DM halos, but SMDS could also form in a variety of halo masses with different final stellar masses. For example, a hydrogen/helium molecular cloud may start to contract in a $10^8\,M_\odot$ halo and produce a DS. Here, the situation is more complicated. The virial temperature of the halo exceeds 10^4 K, the surface temperature we have found for a DS in equilibrium. Hence, it is not clear how accretion onto the DS will proceed. This is the subject of future work. The accretion is expected to be faster due to the increased ambient temperature. We extended our models to $10^8\,M_\odot$ halos in which a more extended period of accretion can lead to SMDS with even larger masses. Tables 3 and 4 show examples of "without" and "with" capture cases, respectively, for $10^8\,M_\odot$ halos. The baryonic mass in the halo is $1.5 \times 10^7\,M_\odot$. Potentially all of this mass could go into the SMDS. Then once the DM runs out it becomes an enormous Population III fusion-powered star, which soon burns out and becomes a BH with mass $> 10^7\,M_\odot$. Such a large BH at early times would clearly help to explain the many large BH found in the universe at early

[7] There is a slight deviation for the $10^3\,M_\odot$ case without capture, where the star is still only 78% radiation pressure supported with the remaining pressure due to gas.

Table 1
Properties and Evolution of Dark Stars for $m_\chi = 100$ GeV, $\dot{M} = 10^{-3}\ M_\odot\ \mathrm{yr}^{-1}$ for the Case "without Capture" but with Extended Adiabatic Contraction

M_* ($M_\odot$)	L_* ($10^6\ L_\odot$)	R_* (AU)	$T_{\rm eff}$ (10^3 K)	ρ_c (g cm^{-3})	T_c (10^5 K)	M_χ ($M_\odot$)	$\rho_{\chi,c}$ (g cm^{-3})	$M_{\rm Ann}$ ($M_\odot$)
10.1	0.13	3.1	4.3	2.8×10^{-7}	1.08	0.02	9.2×10^{-10}	7×10^{-5}
100	1.2	5.2	5.7	7.4×10^{-7}	3.4	0.1	1.5×10^{-9}	5.6×10^{-3}
500	9.7	9.3	7.2	4.3×10^{-6}	8.3	0.5	5.8×10^{-9}	0.26
10^3	17	12	7.5	4.6×10^{-6}	9.8	0.84	3.3×10^{-10}	0.9
10^4	182	18	10.8	1.3×10^{-5}	21	5.3	8.4×10^{-9}	86
10^5	2100	26	16.5	4.1×10^{-5}	46	31.2	1.6×10^{-8}	10750

Notes. The DM halo was taken to be at a redshift of 20 with a concentration parameter of 3.5 and with a mass of $10^6\ M_\odot$. Shown are the stellar mass M_*, the DS luminosity L_*, the stellar radius R_*, the surface temperature $T_{\rm eff}$, the central baryon density ρ_c, the central temperature T_c, the amount of DM in the DS M_χ (due to both adiabatic contraction and capture), the central WIMP density $\rho_{\chi,c}$, and the amount of DM consumed by the DS $M_{\rm Ann}$.

Table 2
Properties and Evolution of Dark Stars for the Case "with Capture," for $m_\chi = 100$ GeV, $\dot{M} = 10^{-3}\ M_\odot\ \mathrm{yr}^{-1}$, and Product of Scattering Cross Section Times Ambient DM Density $\sigma_c \bar{\rho}_\chi = 10^{-39}\ \mathrm{cm}^2 \times 10^{13}$ GeV cm^{-3}

M_* ($M_\odot$)	L_* ($10^6\ L_\odot$)	R_* (AU)	$T_{\rm eff}$ (10^3 K)	ρ_c (g cm^{-3})	T_c (10^5 K)	M_χ ($M_\odot$)	$\rho_{\chi,c}$ (g cm^{-3})	$M_{\rm Ann}$ ($M_\odot$)
10.1	0.13	3.1	4.3	2.8×10^{-7}	1.08	0.02	9.2×10^{-10}	4.0×10^{-5}
100	1.2	5.1	5.7	7.4×10^{-7}	3.5	0.1	1.3×10^{-9}	2.7×10^{-3}
500	5.5	6.0	7.8	1.6×10^{-5}	13	0.3	1.6×10^{-9}	0.09
10^3	8.8	0.3	39	2.9×10^{-1}	390	3.1×10^{-6}	5.4×10^{-7}	0.27
10^4	161	0.9	47	1.1×10^{-1}	440	2.9×10^{-5}	1.1×10^{-6}	77
10^5	1950	2.7	50	3.8×10^{-2}	450	1.3×10^{-4}	3.0×10^{-6}	9900

Notes. The halo has the same parameters as in Table 1. The quantities tabulated are the same as in Table 1. The double horizontal line delineates the transition from adiabatically contracted DM to captured DM once the DS reaches $\sim$1000 $M_\odot$ (after this point, the DM from AC has been annihilated away).

times and today. In addition, since $L_* \propto M_*$, we can predict that the luminosity of the $M_* \sim 10^7\ M_\odot$ SMDSs would be $L_* \sim 10^{11}\ L_\odot$, even easier to detect than a 10^5 SMDS.

It can be seen in Tables 2 and 4 that in the case "with capture" the amount of DM inside the star M_χ is very low at any given moment after the star transitions from adiabatically contracted DM to captured DM. The reason is simple: after a very brief time an equilibrium regime is reached where the annihilation rate is equal to the capture rate. In other words, as soon as a WIMP gets into the DS, it quickly thermalizes and annihilates. This leads to very small amounts of DM inside the star at any one time. Notice, however, that the total amount of DM annihilated (integrated over time) is still very large, as can be seen from the last three entries in the column labeled $M_{\rm Ann}$ of Tables 2–4.

General relativistic instability. The pulsational stability of supermassive stars is an interesting issue. They are radiation pressure dominated with adiabatic index close to $\gamma = 1+1/n = 4/3$, the value that yields neutral stability to radial pulsations for Newtonian bodies with no rotation. Indeed general relativistic corrections (which scale as GM_*/R_*) act in the direction of destabilizing stars and are particularly important for high mass stars. Fowler (1966) examined the stability of supermassive stars using polytropes with $n = 3$ (see Wagoner 1969 for a review). Fowler found that, for the case of no rotation, radial oscillations become dynamically unstable and prevent standard stars more massive than $10^5\ M_\odot$ from reaching a phase of hydrogen burning before collapse. Yet he also found that a small amount of rotation can stabilize the stars, so that rotating stars as heavy as $10^8\ M_\odot$ could be stable en route to reaching hydrogen burning.

In the case of DS, stability to radial pulsations is much easier to achieve. DSs have much larger radii and lower temperatures than fusion-powered stars, so that the general relativistic corrections $\sim GM_*/R_*$ are much smaller. The upper limit on the allowed stellar mass will be larger. In any case, SMDSs are undoubtedly rotating, so that very large stable masses can be achieved (even in the case of rotating ordinary stars, the mass limit is $10^8\ M_\odot$).

In the future, we suggest a stability analysis of our models. The very interesting possibility of short term pulsational instabilities exists, which leads to SMDS as possible standard candles for learning about dark energy or other evolutionary properties of the universe.

4. DETECTABILITY WITH *JWST*

We discuss the capabilities of *JWST* to discover DSs, following the properties of the telescope described by Gardner et al. (2006, 2009). The telescope is designed to be diffraction limited at a wavelength $\lambda_{\rm obs} = 2\,\mu$m. The Near Infrared Camera (NIRCam) will operate in the wavelength range $\lambda = (0.6\text{–}5)\,\mu$m and the Mid-Infrared Camera (MIRI) will operate in the wavelength range $\lambda = 5\text{–}27\,\mu$m. In an exposure of duration 10^4 s, NIRCam will have a limiting sensitivity of 11.4 nJy (1 nJy $= 1 \times 10^{-32}$ erg s^{-1} cm^{-2} Hz^{-1}) in the $2\,\mu$m band, and 13.8 nJy in the $3.5\,\mu$m band and MIRI will have a sensitivity of 700 μJy in the $\lambda = 10\,\mu m$ band (in all cases limiting sensitivities are for a signal-to-noise ratio (S/N) = 10). With longer exposure times, the limiting flux detectable will scale as $\sqrt{t}$ for the same S/N. DS will be characterized by blackbody spectra with surface temperatures $T_{\rm eff} \lesssim 5 \times 10^4$ K. In addition, DSs are also predicted to have hydrogen lines.

We determine the detectability of DSs located at various redshifts $z = 5$, 10, and 15 using the standard Planck spectrum

Table 3
Properties and Evolution of Dark Stars for $m_\chi = 100$ GeV, $\dot{M} = 10^{-1}\ M_\odot\ \mathrm{yr}^{-1}$ for the Case "without Capture" but with Extended Adiabatic Contraction

M_* ($M_\odot$)	L_* ($10^6\ L_\odot$)	R_* (AU)	$T_{\rm eff}$ (10^3 K)	ρ_c (g cm^{-3})	T_c (10^5 K)	M_χ ($M_\odot$)	$\rho_{\chi,c}$ (g cm^{-3})	$M_{\rm Ann}$ ($M_\odot$)
12	0.19	3.6	4.3	1.6×10^{-7}	0.90	0.03	8.4×10^{-10}	1.1×10^{-6}
100	1.9	6.5	5.7	3.8×10^{-7}	2.7	0.2	1.3×10^{-9}	7.6×10^{-5}
10^3	23	15	7.1	2.3×10^{-6}	7.8	1.4	4.0×10^{-9}	1.2×10^{-2}
10^4	172	28	8.6	3.5×10^{-6}	14	9.7	4.3×10^{-9}	0.9
10^5	2100	39	14	1.3×10^{-5}	31	56	9.1×10^{-9}	109
10^6	2.2×10^4	61	19	3.3×10^{-5}	64	355	1.5×10^{-8}	1.1×10^4
10^7	2.2×10^5	97	27	8.3×10^{-5}	127	2200	2.3×10^{-8}	1.2×10^6

Notes. The DM halo was taken to be at a redshift of 15 with a concentration parameter of 3.5 and with a mass of $10^8\ M_\odot$. The quantities tabulated are the same as in Table 1.

Table 4
Properties and Evolution of Dark Stars for the Case "with Capture," for $m_\chi = 100$ GeV, $\dot{M} = 10^{-1}\ M_\odot\ \mathrm{yr}^{-1}$, and Product of Scattering Cross Section Times Ambient DM Density $\sigma_c \bar{\rho}_\chi = 10^{-39}\ \mathrm{cm}^2 \times 10^{13}\ \mathrm{GeV\ cm}^{-3}$

M_* ($M_\odot$)	L_* ($10^6\ L_\odot$)	R_* (AU)	$T_{\rm eff}$ (10^3 K)	ρ_c (g cm^{-3})	T_c (10^5 K)	M_χ ($M_\odot$)	$\rho_{\chi,c}$ (g cm^{-3})	$M_{\rm Ann}$ ($M_\odot$)
11	0.18	3.64	4.3	1.6×10^{-7}	0.9	0.03	8.4×10^{-10}	5.6×10^{-7}
100	1.8	6.5	5.7	3.8×10^{-7}	2.7	0.2	1.3×10^{-9}	3.8×10^{-5}
10^3	22	14	7.2	2.3×10^{-6}	7.8	1.4	3.6×10^{-9}	6.1×20^{-3}
10^4	173	23	9.4	5.8×10^{-6}	16	8.3	2.9×10^{-9}	0.44
4.1×10^4	740	1.8	49	5.7×10^{-2}	444	0.18	7.2×10^{-9}	6.0
10^5	1.9×10^3	2.7	51	3.8×10^{-2}	452	1.3×10^{-4}	2.9×10^{-6}	91
10^6	2.1×10^4	8.5	51	1.2×10^{-2}	456	2.7×10^{-5}	1.5×10^{-4}	1.1×10^4
10^7	2.1×10^5	27	51	3.9×10^{-3}	457	4.0×10^{-10}	1.0×10^2	1.1×10^6

Notes. The DM halo has the same parameters as in Table 3. The quantities tabulated are the same as in Table 1. The double horizontal line delineates the transition from adiabatically contracted DM to captured DM once the DS reaches $\sim 4 \times 10^4\ M_\odot$ (after this point, the DM from AC has been annihilated away).

of blackbody with surface temperature $T_{\rm eff}$ and radius R_* (for DSs similar to those from Tables) in a cosmology with $H_0 = 74$, $\Omega_\Lambda = 0.71$, and $\Omega_M = 0.29$.

Figure 3 shows the observed blackbody flux distribution of two SMDSs formed at $z = 15$ for a WIMP mass $m_\chi = 100$ GeV for the case of extended AC (without capture). The star in the left panel is formed in a $10^6\ M_\odot$ halo and the star in the right panel is formed in a $10^8\ M_\odot$ halo and their stellar (baryonic) masses are $1.7 \times 10^5\ M_\odot$ and $1.5 \times 10^7\ M_\odot$, respectively. Curves are shown assuming the SMDS formed at $z = 15$ and survived to various redshifts, at which it is still producing blackbody radiation. The $1.7 \times 10^5\ M_\odot$ star (left panel) will be detectable by *JWST* (NIRCam) in an exposure of a million seconds, but only if it survives intact till $z = 10$. The $1.5 \times 10^7\ M_\odot$ star (right panel) will be detectable even in a shorter 10^4 s exposure even at $z = 15$ in both the $2\,\mu$m and $3.5\,\mu$m bands. The star on the right may be marginally detectable in a million second exposure in the $10\,\mu$m band of MIRI. The relative flux levels in the three different bands will be important for distinguishing these objects from galaxies.

The curves are not corrected for Lyα absorption by the intergalactic medium (IGM) but the red vertical lines show the location of the 1216 Å line redshifted from the rest-frame wavelength of the star at each of the three redshifts. Flux at wavelengths to the left of the redline at each redshift is expected to be absorbed to some extent by the IGM. Since the surface temperatures of our stars are $\simeq 10^4$ K, the majority of the Lyα absorption ($\lambda_{\rm rest} = 1216$ Å) is expected to occur at wavelengths shorter than that at which the peak flux is emitted. We note that for a DS at $z = 15$ the Lyα absorption line lies at $1.94\,\mu$m—roughly in the middle of the NIRCam $2\,\mu$m band. In this case, the flux in this band will be reduced by about a factor of 2 but will still be well above the detection limit (in 10^6 s). A detailed calculation of the absorption by the IGM is outside the scope of the current paper.

We studied numerous other cases without capture as well: a variety of WIMP masses (10 GeV–2 TeV) as well as various formation redshifts ($z_{\rm form} = 10$–20). We found that DSs with masses up to $M_* \sim 10^5\ M_\odot$ forming in $10^6\ M_\odot$ halos at $z = 20$ and shining at that redshift will in general not be detectable for any value of m_χ (they will become detectable only if they survive to and shine at much lower redshifts).

The smaller DS with $M_* = 800\ M_\odot$ discussed in our previous work (Freese et al. 2008a; Spolyar et al. 2009) will not be visible in *JWST* (see also P. Scott et al. 2010, in preparation); they are several orders of magnitude below the detection limit of *JWST* (in 10^6 s).

Figure 4 shows the observed blackbody flux distribution of two DSs formed at $z = 15$ in halos of two different masses for the case "with capture." Since DSs formed via capture are smaller (in radius) and hotter (than DS formed via extended AC without capture), their peak wavelength tends to shift to lower wavelengths, in some cases out of the range detectable by *JWST*. $10^5\ M_\odot$ stars in $10^6\ M_\odot$ halos are only detectable if they survive until $z = 5$ at which time they could be detectable in a long (10^6 s exposure). On the other hand, $10^7\ M_\odot$ stars formed in $10^8\ M_\odot$ halos will be easily detectable even in an exposure of 10^4 s all the way out to $z = 15$. For most other WIMP masses and formation redshifts, DSs formed in $10^6\ M_\odot$ halos via capture are below the detection limit of *JWST*.

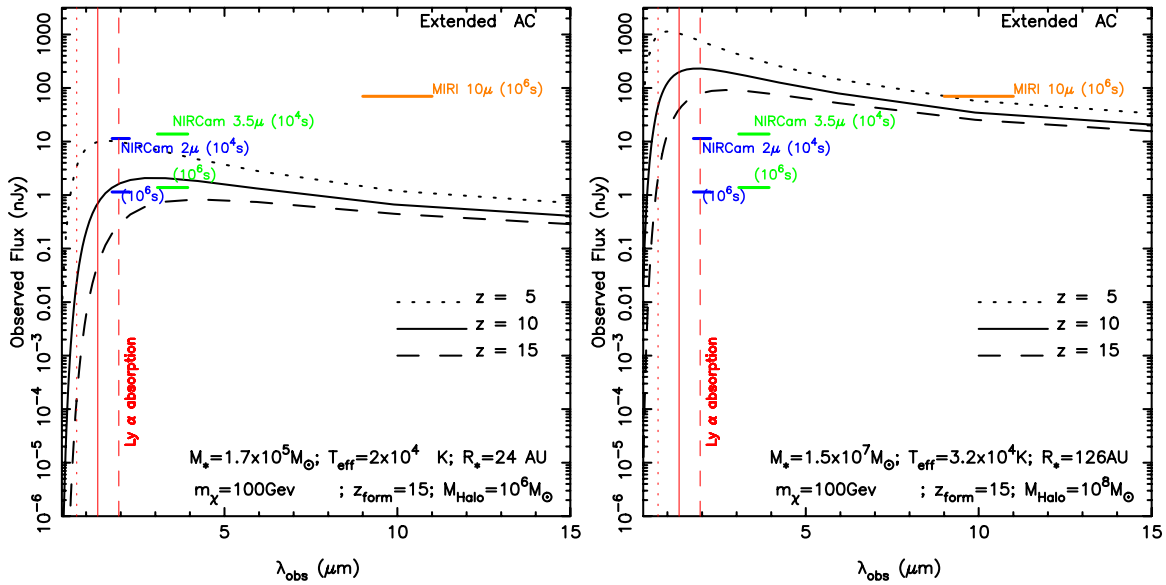

Figure 3. Blackbody spectra of two dark stars (DSs) formed via extended adiabatic contraction ("without capture") for $m_\chi = 100$ GeV. Left panel: $1.7 \times 10^5\ M_\odot$ SMDS in a $10^6\ M_\odot$ halo. Right panel: $1.5 \times 10^7\ M_\odot$ SMDS in $10^8\ M_\odot$ halo. The blackbody flux is shown at $z = 15$ (formation redshift) and at $z = 10$ and 5 (see line legends) assuming that the DS survives till the lower redshifts. Blue dashes show sensitivity limit and bandwidth of NIRCam 2μ ($R = 4$) while the green dashes show the sensitivity limit and band width of the NIRCam 3.5μ ($R = 4$) band. The upper and lower dashes show the sensitivity limits after exposure times of 10^4 s, 10^6 s, respectively. The sensitivity of MIRI (10μ, $R = 5$) is shown for exposure time of 10^6 s (orange dash). All sensitivities are computed assuming an S/N = 10. The red vertical lines show the location of the 1216 Å line redshifted from the rest-frame wavelength of the star at each of the three redshifts. The observed flux to the left of the vertical lines will decrease relative to the black curves depending on the model assumed for IGM absorption up to the redshift of reionization.

(A color version of this figure is available in the online journal.)

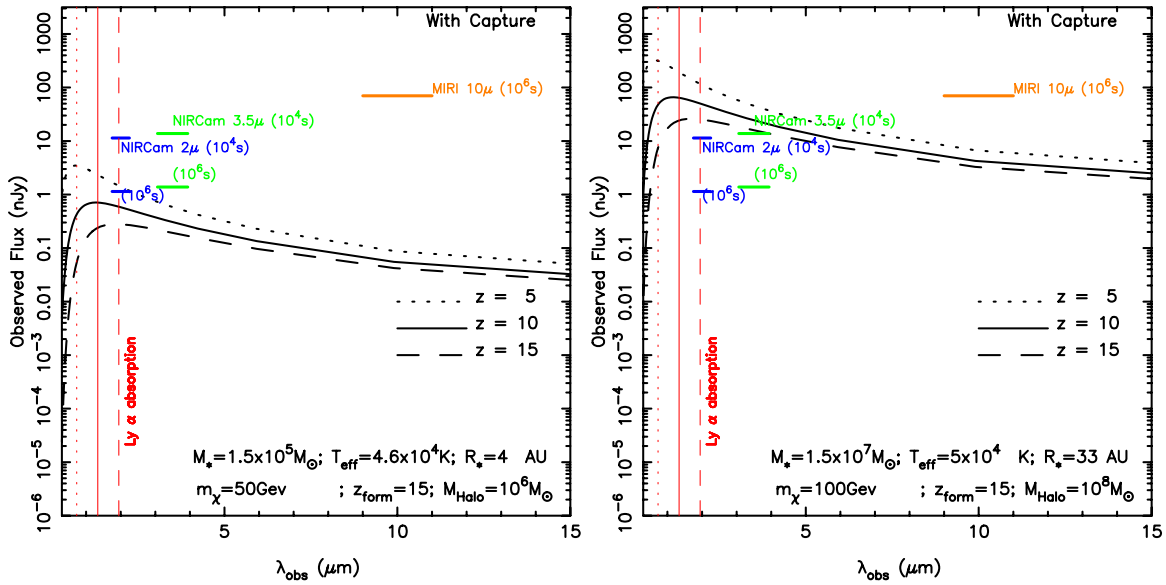

Figure 4. Similar to Figure 3 but for dark stars formed "with capture." Left panel: $1.7 \times 10^5\ M_\odot$ SMDS formed in $10^6\ M_\odot$ halo ($m_\chi = 50$ GeV). Right panel: $1.7 \times 10^7\ M_\odot$ SMDS formed in $10^8\ M_\odot$ halo ($m_\chi = 100$ GeV).

(A color version of this figure is available in the online journal.)

The prospect of detecting SMDS in *JWST* and confirming the existence of a new phase of stellar evolution is exciting. In the most optimistic cases, detection in a number of different wavelength bands could be used to obtain a spectrum and differentiate these DSs from galaxies or other sources.

5. CONCLUDING REMARKS

Using our polytropic model for DSs, we have considered accretion of baryonic matter onto the DS as they become supermassive, $M_* > 10^5\ M_\odot$. Such large masses are possible because the DS is cool enough (as long as it is powered by DM) so that radiative feedback effects from the star do not shut off the accretion of baryons, as long as it is powered by DM. We considered two different scenarios for supplying the required amount of DM.

1. *The case of extended AC, labeled "without capture" in the figures.* In this case, DM is supplied by the gravitational attraction of the baryons in the star. In triaxial halos, DM orbits are quite complex and the DM in the core is harder to deplete than previously estimated. This case does *not*

include any captured DM, and relies solely on the particle physics of WIMP annihilation. To grow to a $10^5\ M_\odot$ SMDS in a $10^6\ M_\odot$ halo, or to grow to a $10^7\ M_\odot$ SMDS in a $10^8\ M_\odot$ halo, the amount of DM consumed can be as much as ∼1% of the total DM in the halo (depending on the accretion rate). This amount is not unreasonable, since Valluri et al. (2010) found that the fraction of box and chaotic DM orbits is as high as 85% in triaxial halos and remains over 10% when a significant compact baryonic component causes the halo to become axisymmetric at small radii. Future work will be required to accurately obtain WIMP orbits, densities, and timescales (work in progress). For now, we took the simplistic approach of using our previous prescription for AC in a spherical potential but not removing the annihilated DM.

2. *The case of extended capture, labeled "with capture" in the figures.* Here, the original DM inside the star from AC is assumed to be depleted after ∼ 300,000 yr, then the star begins to shrink somewhat, and capture of DM from the surroundings takes place as it scatters elastically off of nuclei in the star. In this case, the additional particle physics ingredient of WIMP scattering is required.

In this paper, we studied the formation of $10^5\ M_\odot$ SMDS in $10^6\ M_\odot$ DM halos and $10^7\ M_\odot$ SMDS in $10^8\ M_\odot$ halos. These stars become very bright, $L_* \sim (10^9$–$10^{11})\ L_\odot$. Figure 1 shows the H–R diagram for a variety of WIMP masses, and follows the DS as it climbs up to ever higher masses. They live millions to billions of years, depending on the merger history with other halos. Once the DM runs out, the SMDSs have brief lives as fusion-powered Population III stars before collapsing into $> 10^5\ M_\odot$ BHs, possible seeds for many of the big BH seen in the universe today and at early times. A proper study of the final mass of the DS and resultant BH will depend on cosmological simulations. The original halo containing the DS will merge with other halos. No one knows what exactly will happen to the DM density in the vicinity of the DS when this happens. The DS could end up even more massive. DS may also form in larger halos that form at later times, as long as the baryonic content is still only H and He. Localized regions with this property could exist even at redshifts $z < 7$ (Furlanetto & Loeb 2005; Choudhury & Ferrara 2007).

SMDS would make plausible precursors of the $10^9\ M_\odot$ BHs observed at $z > 6$ (Fan et al. 2004; Li et al. 2007) of intermediate mass BHs; of BH at the centers of galaxies; and of the BH inferred by extragalactic radio excess seen by the ARCADE experiment (Seiffert et al. 2009). In addition, the formation of BH from DS could be accompanied by high-redshift gamma ray bursts thought to take place due to the gravitational collapse of supermassive stars.

In the future, we suggest a stability analysis of our models. The very interesting possibility of short term pulsational instabilities exists, which leads to SMDS as possible standard candles for learning about dark energy or other evolutionary properties of the universe.

SMDSs could be detected by *JWST* for a variety of parameter ranges. These are extremely bright objects $L_* \sim (10^9$–$10^{11})\ L_\odot$ and yet are very cool $T \sim 10{,}000$ K, so that their emitted light is in the wavebands detectable by *JWST*. The longer they live, the more easy they are to detect. Figures 3 and 4 give examples of what one could look for in *JWST*. For the most optimistic cases, one could even test for the blackbody spectrum in a number of different wavebands. In principle, hydrogen or helium lines could be found to complement the blackbody emission. If, in addition, someday high energy neutrinos are found to emanate from these stars, then it will be a clincher that DM annihilation took place inside the DS.

It is interesting to speculate that the initial mass function of Population III fusion-powered stars may be determined by the cutoff of the DM supply, which may vary from one DS to another. DSs continue to accrete mass as long as the DM annihilation powers the star and keeps it cool enough. Once the DM fuel supply is exhausted, the star shrinks and heats up, fusion begins, and the mass growth of the star is quickly halted due to feedback from hot emitted photons. Hence, the details of the cutoff of the DM supply may determine the sizes of Population III stars entering the fusion era. The cutoff will take place at different DS masses in different halos, depending on the details of the cosmological merger history. Different final DS masses may result for different individual DS depending on the evolution of their parent halos.

After the submission of this paper, we became aware of another paper which discusses the prospects of detecting DSs with masses up to $\simeq 800\ M_\odot$ with *JWST*, Zackrisson et al. (2010). This paper considers the possibility that DSs might be detected individually if their flux is magnified by a foreground gravitational lensing cluster. These authors also show that the stellar atmospheres can quite significantly modify the observed spectral energy distributions of DSs due to the Balmer break for DSs with surface temperatures less than ∼6000 K but that these effects are relatively weak for $T_{\rm eff} \gtrsim 10^4$ K. Since most of our SMDSs are in fact hotter than 10^4 K, we expect that our blackbody spectra are quite a good approximation to the observable spectral energy distributions. Zackrisson et al. (2010) also demonstrate that if DSs live for $\gtrsim 10^7$yr, even a small fraction (0.7%)of such stars in a protogalactic star cluster at $z \sim 10$ would result in a significantly redder color of this object and that it would be clearly distinguishable from a normal star forming galaxy, active galactic nucleus at high redshift, as well as from foreground brown dwarfs and cool stars in the Milky Way.

We acknowledge support from the DOE and MCTP via the University of Michigan (K.F. and C.I.), DOE at Fermilab (D.S.), and the NSF grant AST-0908346 (M.V). K.F. is grateful to M. Begelman, W. Freedman, J. Friedman, O. Gnedin, B. O'Shea, B. Schmidt, P. Shapiro, T. Tyson, and S. White for helpful discussions. We thank Jon Gardner for very helpful comments regarding *JWST*.

REFERENCES

Abdo, A. A., et al. (The Fermi LAT Collaboration) 2009, Phys. Rev. Lett., 102, 181101
Adriani, O., et al. (*PAMELA* Collaboration) 2009, Nature, 458, 607
Ahmed, Z., et al. (The CDMS-II Collaboration) 2009, arXiv:0912.3592
Allgood, B., Flores, R. A., Primack, J. R., Kravtsov, A. V., Wechsler, R. H., Faltenbacher, A., & Bullock, J. S. 2006, MNRAS, 367, 1781
Bahcall, J. N. 1989, Neutrino Astrophysics (Cambridge: Cambridge Univ. Press)
Bailin, J., & Steinmetz, M. 2005, ApJ, 627, 647
Bardeen, J. M., Bond, J. R., Kaiser, N., & Szalay, A. S. 1986, ApJ, 304, 15
Barkana, R., & Loeb, A. 2001, Phys. Rep., 349, 125
Barnes, J., & Efstathiou, G. 1987, ApJ, 319, 575
Barnes, J., & White, S. D. M. 1984, MNRAS, 211, 753
Begelman, M. 2009, arXiv:0910.4398
Bernabei, R., et al. (DAMA collaboration) 2010, in AIP Conf. Proc. 1223, Science with the New Generation of High Energy Gamma Ray-Experiments: Proc. 7th Workshop on Gamma-Ray Physics in the LHC Era, ed. C. Cecchi et al. (Melville, NY: AIP), 50
Bertone, G., & Fairbairn, M. 2007, arXiv:0711.1485

Binney, J., & Tremaine, S. 2008, Galactic Dynamics (2nd ed.; Princeton, NJ: Princeton Univ. Press)
Blumenthal, G. R., Faber, S. M., Flores, R., & Primack, J. R. 1986, ApJ, 301, 27
Bouquet, A., & Salati, P. 1989, ApJ, 346, 284
Bromm, V., & Larson, R. B. 2004, ARA&A, 42, 79
Choudhury, T. P., & Ferrara, A. 2007, MNRAS, 380, 6
de Zeeuw, T. 1985, MNRAS, 216, 273
Debattista, V. P., Moore, B., Quinn, T., Kazantzidis, S., Maas, R., Mayer, L., Read, J., & Stadel, J. 2008, ApJ, 681, 1076
Dobler, G., Finkbeiner, D. P., Cholis, I., Slatyer, T. R., & Weiner, N. 2009, arXiv:0910.4583
Dubinski, J. 1994, ApJ, 431, 617
Dubinski, J., & Carlberg, R. G. 1991, ApJ, 378, 496
Evrard, A. E., Summers, F. J., & Davis, M. 1994, ApJ, 422, 11
Fan, X., et al. 2001, AJ, 121, 31
Fan, X., et al. 2004, AJ, 128, 515
Fan, X., et al. 2006, AJ, 131, 1203
Fowler, W. A. 1966, ApJ, 144, 180
Freese, K., Bodenheimer, P., Spolyar, D., & Gondolo, P. 2008a, ApJ, 685, L101
Freese, K., Gondolo, P., Sellwood, J. A., & Spolyar, D. 2009, ApJ, 693, 1563
Freese, K., Spolyar, D., & Aguirre, A. 2008b, J. Cosmol. Astropart. Phys., JCAP11(2008)014
Frenk, C. S., White, S. D. M., Davis, M., & Efstathiou, G. 1988, ApJ, 327, 507
Furlanetto, S. R., & Loeb, A. 2005, ApJ, 634, 1
Gardner, J. P., et al. 2006, Space Sci. Rev., 123, 485
Gardner, J. P., et al. 2009, in Astrophysics and Space Science Proceedings, Astrophysics in the Next Decade, ed. H. A. Thronson, M. Stiavelli, & A. G. G. M. Tielens (Springer: Netherlands), 1
Gerhard, O. E., & Binney, J. 1985, MNRAS, 216, 467
Goodman, J., & Schwarzschild, M. 1981, ApJ, 245, 1087
Graff, D. S., & Freese, K. 1996, ApJ, 467, L65
Heger, A., & Woosley, S. E. 2002, ApJ, 567, 532
Hoyle, F., & Fowler, W. 1963, MNRAS, 125, 169
Iglesias, C. A., & Rogers, F. J. 1996, ApJ, 464, 943
Iocco, F. 2008, ApJ, 667, L1
Iocco, F., Bressan, A., Ripamonti, E., Schneider, R., Ferrara, A., & Marigo, P. 2008, MNRAS, 390, 1655
Jing, Y. P., & Suto, Y. 2002, ApJ, 574, 538
Kazantzidis, S., Kravtsov, A. V., Zentner, A. R., Allgood, B., Nagai, D., & Moore, B. 2004, ApJ, 611, L73
Kippenhahn, R., & Weigert, A. 1990, Stellar Structure and Evolution (Berlin: Springer)
Krauss, L., Freese, K., Press, W., & Spergel, D. N. 1985, ApJ, 299, 1001
Lenzuni, P., Chernoff, D. F., & Salpeter, E. 1991, ApJS, 76, 759
Li, Y. X., et al. 2007, ApJ, 665, 187
Magorrian, J., & Tremaine, S. 1999, MNRAS, 309, 447
McKee, C. F., & Tan, J. C. 2008, ApJ, 681, 771
Merritt, D., & Fridman, T. 1996, ApJ, 460, 136
Merritt, D., & Poon, M. Y. 2004, ApJ, 606, 788
Merritt, D., & Quinlan, G. D. 1998, ApJ, 498, 625
Merritt, D., & Valluri, M. 1996, ApJ, 471, 82
Moskalenko, I. V., & Wai, L. L. 2007, ApJ, 659, L29
Natarajan, A., Tan, J. C., & O'Shea, B. W. 2009, ApJ, 692, 574
O'Shea, B. W., & Norman, M. L. 2007, ApJ, 654, 66
Ripamonti, E., & Abel, T. 2005, arXiv:astro-ph/0507130
Ripamonti, E., Iocco, F., Ferrara, A., Schneider, R., Bressan, A., & Marigo, P. 2010, arXiv:1003.0676
Ripamonti, E., Iocco, F., Bressan, A., Schneider, R., Ferrara, A., & Marigo, P. 2009, in Proc. of Science, Identification of Dark Matter 2008 (Trieste: SISSA), PoSIDM2008:075, 2009
Ryden, B. S., & Gunn, J. E. 1987, ApJ, 318, 15
Salati, P., & Silk, J. 1989, ApJ, 338, 24
Schleicher, D., Banerjee, R., & Klessen, R. 2008, Phys. Rev. D, 78, 083005
Schleicher, D., Banerjee, R., & Klessen, R. 2009, Phys. Rev. D, 79, 043510
Schwarzschild, M. 1979, ApJ, 232, 236
Schwarzschild, M. 1993, ApJ, 409, 563
Scott, P., Edsjo, J., & Fairbairn, M. 2007, arXiv:0711.0991
Scott, P., Fairbairn, M., & Edsjo, J. 2009, MNRAS, 394, 82
Seiffert, M., et al. 2009, arXiv:0901.0559
Spolyar, D., Bodenheimer, P., Freese, K., & Gondolo, P. 2009, ApJ, 705, 1031
Spolyar, D., Freese, K., & Gondolo, P. 2008, Phys. Rev. Lett., 100, 051101
Tan, J. C., & McKee, C. F. 2004, ApJ, 603, 383
Taoso, M., Bertone, G., Meynet, G., & Ekström, S. 2008, Phys. Rev. D., 78, 123510
Tissera, P. B., White, S. D. M., Pedrosa, S., & Scannapieco, C. 2009, arXiv:0911.2316
Umeda, H., Yoshida, N., Nomoto, K., Tsuruta, S., Sasaki, M., & Ohkubo, T. 2009, J. Cosmol. Astropart. Phys., JCAP08(2009)024
Valluri, M., Debattista, V. P., Quinn, T., & Moore, B. 2010, MNRAS, 403, 525
Valluri, M., & Merritt, D. 1998, ApJ, 506, 686
Wagoner, R. V. 1969, ARA&A, 7, 553
Yoon, S.-C., Iocco, F., & Akiyama, S. 2008, ApJ, 688, L1
Yoshida, N., Abel, T., Hernquist, L., & Sugiyama, N. 2003, ApJ, 592, 645
Zackrisson, E., et al. 2010, arXiv:1002.3368